

# A SIMPLIFIED APPROACH FOR CLOSED-LOOP SPEED CONTROL OF A DC MOTOR USING AC-TO-DC CONVERTER

S.S. Shokralla

Electrical Engineering Department, Faculty of Engineering,  
Menoufiya University, Shebin El-Kom, Egypt.

## ABSTRACT

In this paper a simplified approach for speed control of a separately excited DC motor using single-phase, single-way rectifier is introduced. The strategy of this approach is based on the cascade combination of diode bridge rectifier and Cuk converter. Step-up and step-down characteristics of the output voltage can be obtained. The supply current appears to be approximately sinusoidal with a relatively high power factor. A high performance is achieved with a simple control circuit having only one switch for the converter. The simulation program is performed using the differential equations describing the system in different modes of operation. The program is adapted to predict the steady-state and dynamic behaviour. The transfer function as well as the P.I. controller parameters of the system are obtained from simulation results. The P.I. parameters are selected from an overview of practical experience to satisfy the best required response for load, speed reference and supply input voltage disturbances. The simulation results for both open and closed loop speed control system are given and proved to yield good agreement when compared with the experimental results.

*Keywords: Separately excited d.c. motor, Closed-loop speed control, AC-to-DC converter.*

## Nomenclature

B	Viscous friction coefficient
C	Energy storage / transfer capacitance.
$C_o$	Capacitance of the filter capacitor
e	Capacitor voltage
f	Supply frequency
$f_s$	Switching frequency
$i_m$	Instantaneous armature current
$i_s$	Instantaneous supply current
J	Moment of inertia
$K_m$	Back e.m.f. coefficient
$K_t$	Tacho-generator constant
$L_a, R_a$	Armature inductance and resistance
$L_1, r_1$	Inductance and resistance of the coil connected with bridge rectifier.
$L_2, r_2$	Filter inductance and resistance
$R_f$	Field resistance
$T_L$	Load torque
U	Integrator output
v, V	Instantaneous and peak values of supply input voltage
$V_c$	Control voltage

$V_o$	D.C. output voltage
$\omega$	Supply angular velocity
$\omega_m$	Motor angular velocity
$\tau_1, K_1$	Controller parameters

## 1. INTRODUCTION

Power supplies suffer from current distortions and low power factor operations. This is due to employing a conventional single-phase voltage source diode rectifier with a filter capacitor at the output terminal and also the phase controlled rectifiers. In order to overcome these disadvantages, various circuit topologies using power switching devices, such as Gate turn off thyristors, power transistors, MOSFET'S and IGBT'S ac-to-dc converters have been implemented to obtain high power factor and minimum current distortions with static loads [1-7].

The basic step-down/up switching regulator is known as buck-boost converter, the output voltage

of such converter can be either higher or lower than the input voltage. The disadvantage of buck-boost converter is that both the input current and the current feeding the output stage are highly discontinuous which leads to a large external filtering requirements [8].

Many boost and Cuk-type converters have been presented using hysteresis control to achieve high power factor and minimum current distortions. According to boost - type converters, the output d.c. voltage can only be higher than the input a.c. source voltage [9]. A Cuk-type converter is able to step-up or step down switching regulator. An advantage of this converter is that both the input current and the current feeding the output stage are reasonably ripple free. Nevertheless, there are still some disadvantages, such as requiring complicated control circuit and nonfixed switching frequency [10-12].

Implementation of a DC motor supplied from single-phase rectifier with boost type converter has been investigated in Reference [13]. No attention has been paid to the transient performance and the speed control of the motor was done for open loop, only.

In this paper, a simple ac-to-dc CuK converter feeding separately excited dc motor is presented. This technique is performed without using a current sensor, using simple control circuit with step-up/down capability. Only one switch is employed for this converter and approximately unity power factor can be obtained as well as the motor voltage and current are reasonably ripple free.

The digital simulation for open and closed loop speed control system has been given. The proposed simulation enables to compute the best controller parameters for transient response. Although the load has been disturbed within the range  $\pm 25\%$  of its rated value, the motor speed appears to be consistent and remain constant. Also, the speed response due to a step change in the reference speed is fast with reasonable overshoot. Moreover, when the input voltage is disturbed within the range  $\pm 15\%$  of the applied voltage, the speed of the motor is found to be constant.

Finally, the simulation results are in good agreement when compared with the experimental values.

## 2. DESCRIPTION OF THE EXPERIMENTAL EQUIPMENT

Figure (1) shows the schematic diagram of the complete control system for speed control. The system consists of a cascade combination of diode bridge rectifier and Cuk converter connected to AC single-phase supply. Step-up and step-down behaviour of the output voltage is obtained by regulating the control voltage ( $V_c$ ) from 0 to maximum value ( $A$ ) of the timing voltage ( $\omega_a$ ) shown in Figure (2). This technique has been used to control the motor speed. Capacitor  $C$  acts as an energy storage/transfer element. The inductance  $L_2$  and the capacitor  $C_o$  are used as a d.c. filter to obtain smooth and ripple free output dc voltage.

The MOSFET (type IRFP 450) is fired by an impulse generator having linear timing voltage. The gate pulses are generated such that the control voltage ( $V_c$ ) equals the timing voltage ( $\omega_a$ ) as shown in Figure (2). Control of motor speed is performed using proportional integral (P.I.) controller. The switching frequency ( $f_s$ ) is set to 2.2 K.Hz. This value has been selected to be greater than the low pass filter ( $L_2, C_o$ ) corner frequency as well as resonance frequency ( $f_r$ ). The greater value of  $f_s$  should be chosen out of the audible frequency range.

The parameters of the power circuit is determined according to the range of the switching frequency and acceptable percentage of the output ripple. The rate of change of  $i_1$ , switching frequency and value of  $C$  are determined by the value of  $L_1$ . The resonant frequency is given by  $f_r = (1/2\pi) (L_1 C)^{-0.5}$  and should be sufficiently lower than the switching frequency ( $f_s = 1/T$ ) to prevent any resonant phenomenon in the AC circuit. The corner frequency of the low-pass filter is selected to be much lower than the switching frequency, thus essentially eliminating the switching frequency ripple in the output voltage. The higher values of  $L_2$  and  $C_o$  assign the better output of voltage and current but on the expense of the system time response. The parameter values of the designed system are given in Appendix [1].

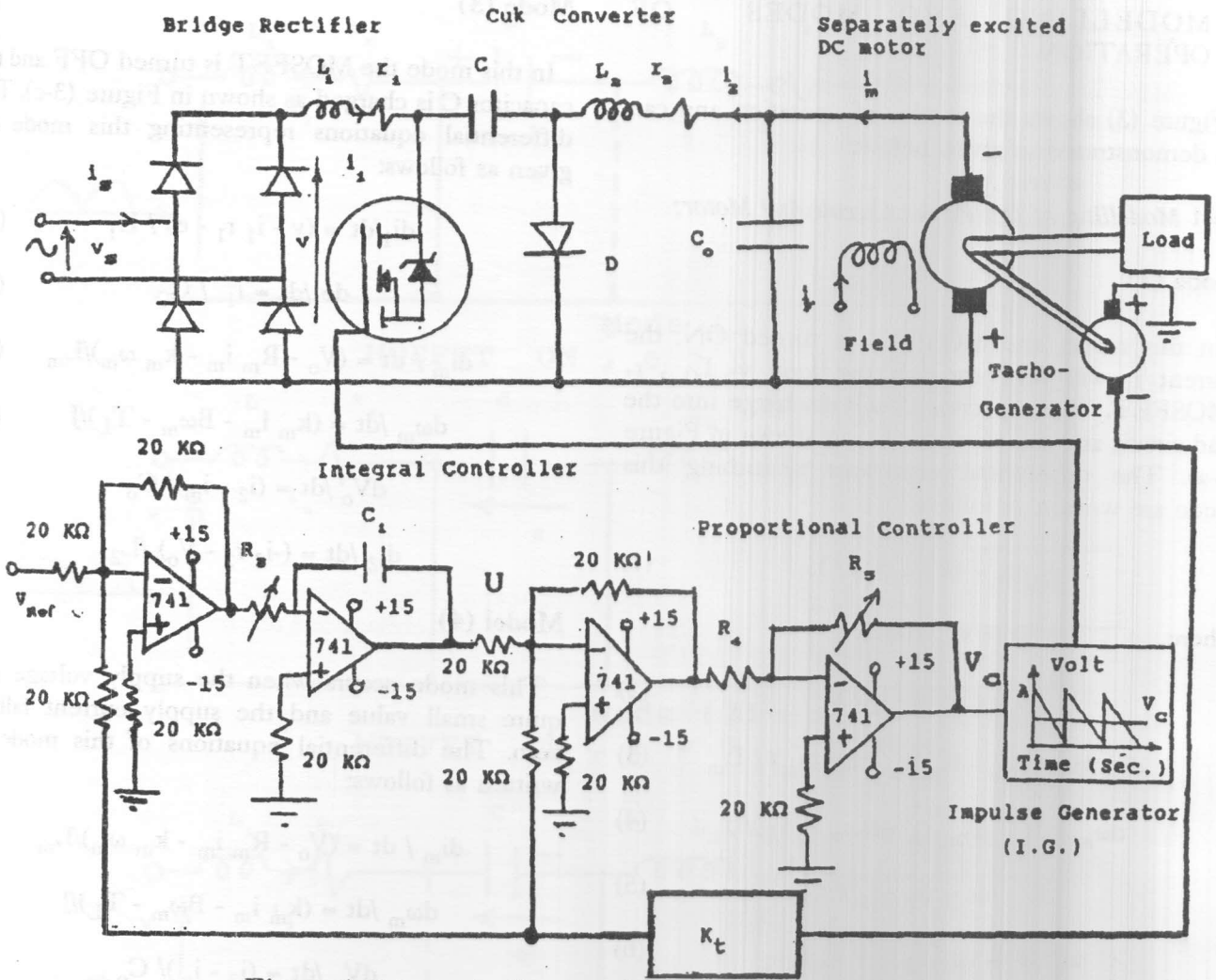


Figure 1. Schematic diagram of the experimental system.

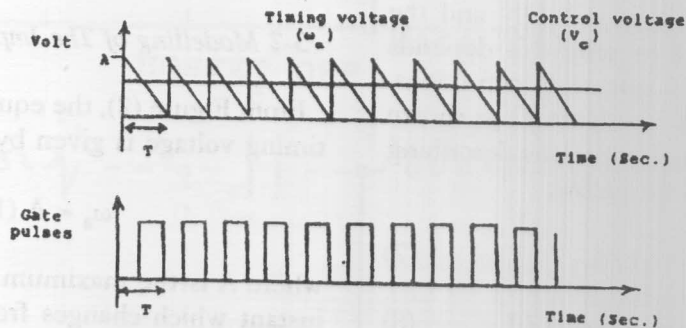


Figure 2. Output of the drive and control circuit.

### 3. MODELLING AND MODES OF OPERATION

Figure (3) shows the modes of operation and can be demonstrated as given below:

#### 3-1 Modelling of The Power Circuit And Motor:

##### Mode (1)

In this mode, the MOSFET is turned ON, the current  $i_1$  will flow through the loop  $v - L_1, r_1$  -MOSFET. The capacitor C will discharge into the load circuit and the capacitor  $C_o$  as shown in Figure (3-a). The differential equations describing this mode are written as follows:

$$di_1/dt = (v - i_1 r_1) / L_1 \quad (1)$$

where,  $v = V | \sin \omega t |$

$$de / dt = - i_2 / C \quad (2)$$

$$di_m / dt = (V_o - R_m i_m - k_m \omega_m) / L_m \quad (3)$$

$$d\omega_m / dt = (K_m i_m - B\omega_m - T_L) / J \quad (4)$$

$$dV_o / dt = (i_2 - i_m) / C_o \quad (5)$$

$$di_2 / dt = (e - i_2 r_2 - V_o) / L_2 \quad (6)$$

##### Mode (2)

In this mode, the MOSFET is still ON and the capacitor voltage (e) may fall to zero, this depends on the circuit parameters and operating conditions. The current  $i_2$  will circulates via diode D as shown in Figure (3-b). The differential equations describing this mode may written as given below:

$$di_1/dt = (v - i_1 r_1) / L_1 \quad (7)$$

$$di_m / dt = (V_o - R_m i_m - k_m \omega_m) / L_m \quad (8)$$

$$d\omega_m / dt = (K_m i_m - B\omega_m - T_L) / J \quad (9)$$

$$dV_o / dt = (i_2 - i_m) / C_o \quad (10)$$

$$di_2 / dt = (-i_2 r_2 - V_o) / L_2 \quad (11)$$

In this mode the MOSFET is turned OFF and the capacitor C is charged as shown in Figure (3-c). The differential equations representing this mode are given as follows:

$$di_1/dt = (v - i_1 r_1 - e) / L_1 \quad (12)$$

$$de / dt = i_1 / C \quad (13)$$

$$di_m / dt = (V_o - R_m i_m - k_m \omega_m) / L_m \quad (14)$$

$$d\omega_m / dt = (k_m i_m - B\omega_m - T_L) / J \quad (15)$$

$$dV_o / dt = (i_2 - i_m) / C_o \quad (16)$$

$$di_2 / dt = (-i_2 r_2 - V_o) / L_2 \quad (17)$$

##### Model (4)

This mode occurs when the supply voltage is of quite small value and the supply current falls to zero. The differential equations of this mode are written as follows:

$$di_m / dt = (V_o - R_m i_m - k_m \omega_m) / L_m \quad (18)$$

$$d\omega_m / dt = (k_m i_m - B\omega_m - T_L) / J \quad (19)$$

$$dV_o / dt = (i_2 - i_m) / C_o \quad (20)$$

$$di_2 / dt = (-i_2 r_2 - V_o) / L_2 \quad (21)$$

#### 3-2 Modelling of The Impulse Generator

From Figure (2), the equation which represents the timing voltage is given by the following expression:

$$\omega_a = A (1.0 - X/T) \quad (22)$$

where A is the maximum voltage (12 volt), X is any instant which changes from 0 to  $2\pi$  in radians and T is the chopping period in radians which can be given by:

$$T = \omega (1 / f_s) \quad (23)$$



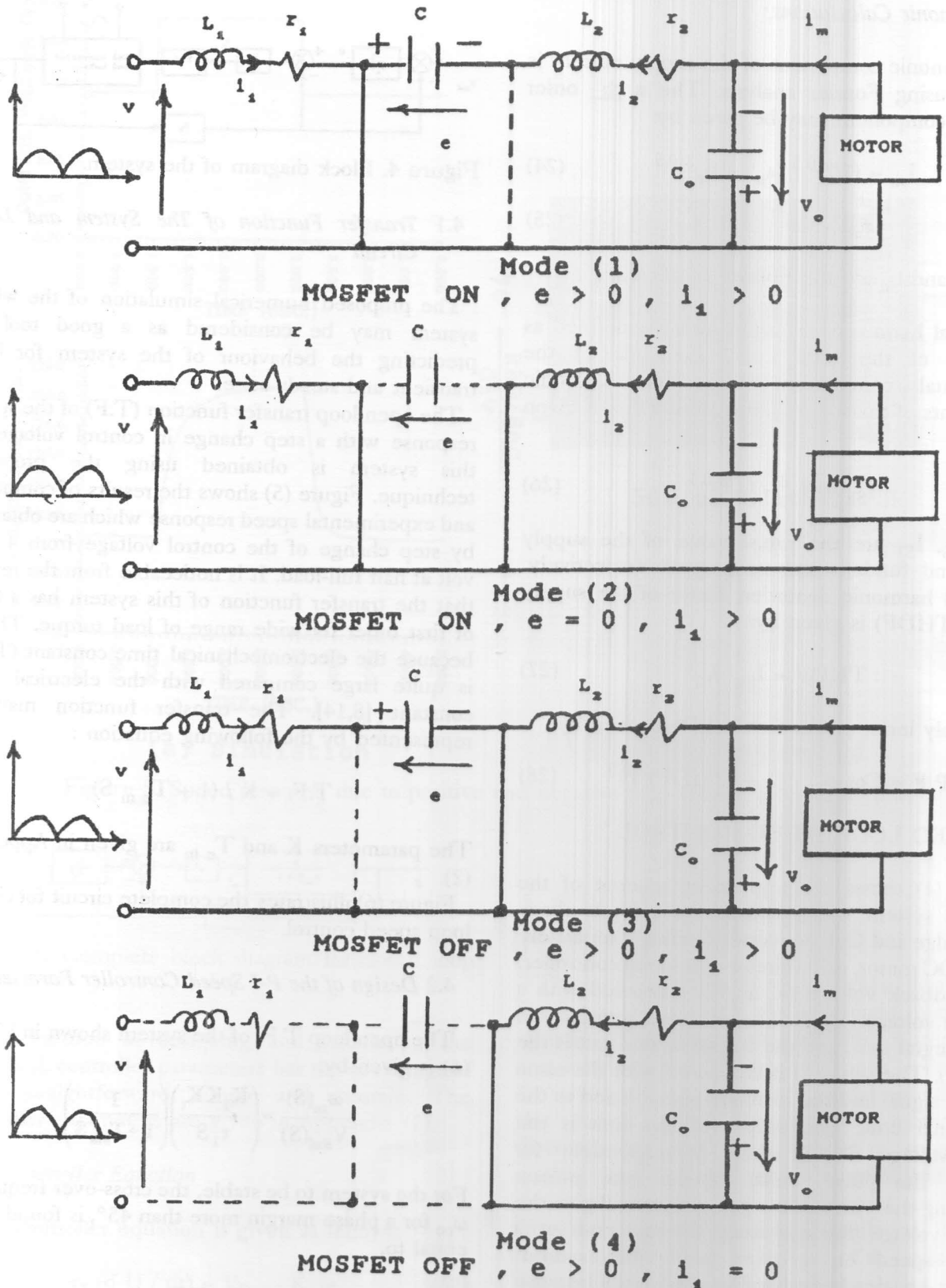


Figure 3. Modes of operation for the system.

3.3 Harmonic Calculations:

The harmonic component of the supply current is obtained using Fourier analysis. The  $n^{th}$  order harmonic component may be given by:

$$I_{sn} = (1/2)^{0.5} (a_n^2 + b_n^2)^{0.5} \quad (24)$$

$$\phi_{sn} = \tan^{-1} (a_n/b_n) \quad (25)$$

where  $a_n$  and  $b_n$  are the Fourier coefficients.

The total harmonic distortion factor is defined as the ratio of the total r.m.s. harmonic to the fundamental component. The total harmonic components of the supply input current  $I_{Sh}$  is given by:

$$I_{Sh} = (I_S^2 - I_{S1}^2)^{0.5} \quad (26)$$

where,  $I_S, I_{S1}$  are the r.m.s. value of the supply current and fundamental component respectively. The total harmonic distortion factor of the supply current (THDF) is given by:

$$THDF = I_{Sh} / I_{S1} \quad (27)$$

The supply input power factor (PF) is given by:

$$P F = \text{Cos } \phi_{S1} / [1 + (THDF)^2]^{0.5} \quad (28)$$

4. CLOSED LOOP SPEED CONTROL

Figure (4) shows the equivalent scheme of the complete system which consists of a single-phase diode bridge and Cuk-converter feeding a separately excited DC motor, drive circuit and speed controller. The Feedback voltage ( $k_t \omega_m$ ) is compared with a reference voltage ( $V_{Ref}$ ). The resultant signal is fed to the integral unit, and the output of this unit is the signal (U). The signal U is compared with the same feedback signal and the resultant signal is fed to the proportional unit. The output of this unit is the control voltage ( $V_C$ ) which is responsible for changing the pulse width of the gate pulses. Controlling the width of the gate pulses will give the suitable voltage for operating the machine at a constant speed on a given load. The current controller has not been used in this paper because the power of the employed machine is small.

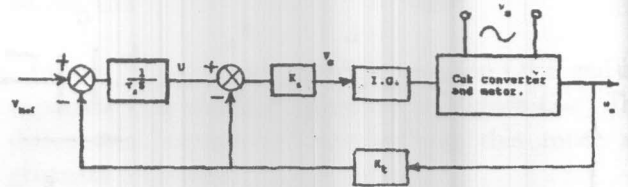


Figure 4. Block diagram of the system.

4.1 Transfer Function of The System and Drive Circuit

The proposed numerical simulation of the whole system may be considered as a good tool for predicting the behaviour of the system for both transient and steady-state.

The open loop transfer function (T.F) of the speed response with a step change in control voltage for this system is obtained using the proposed technique. Figure (5) shows the results of computed and experimental speed response which are obtained by step change of the control voltage from 4 to 8 volt at half full-load. It is noticeable from the results that the transfer function of this system has a form of first order for wide range of load torque. This is because the electromechanical time constant ( $T_{em}$ ) is quite large compared with the electrical time constant [8,14]. The transfer function may be represented by the following equation :

$$T.F. = K / (1 + T_{em} S) \quad (29)$$

The parameters  $K$  and  $T_{em}$  are given in Appendix (2).

Figure (6) illustrates the complete circuit for closed loop speed control.

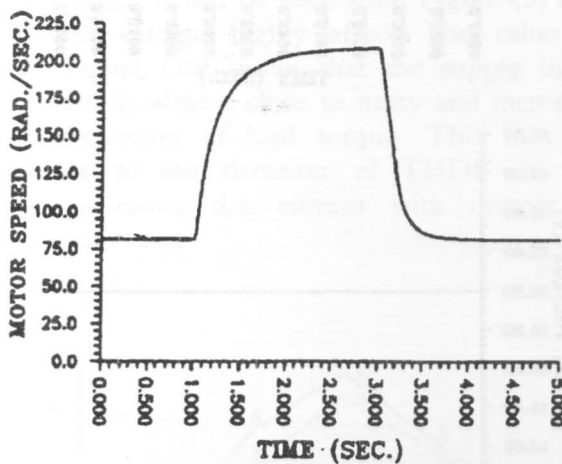
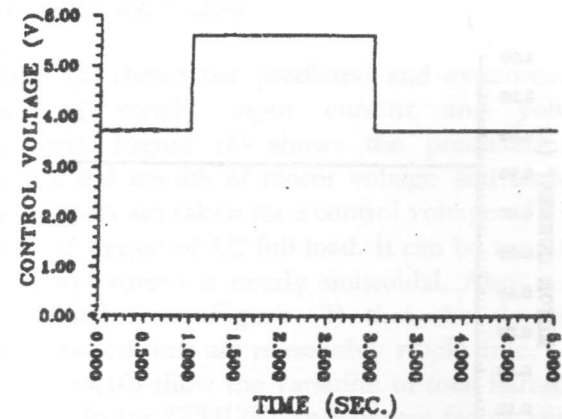
4.2 Design of the P-I Speed Controller Parameters:

The open loop T.F. of the system shown in Figure (6) is given by:

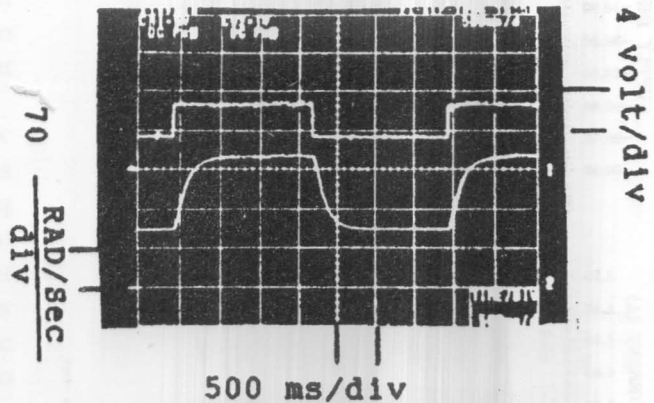
$$\frac{\omega_m(S)}{V_{Ref}(S)} = \left( \frac{K_1 K K_t}{\tau_1 S} \right) \left( \frac{1}{1 + T_{em} S} \right) \quad (30)$$

For the system to be stable, the cross-over frequency  $\omega_{co}$  for a phase margin more than  $45^\circ$ , is found to be equal to,

$$\omega_{co} = K_1 K K_t / \tau_1 \quad (31)$$



(a) Simulation



(b) Experimental .

Figure 5. Speed response due to positive and negative step change in control voltage.

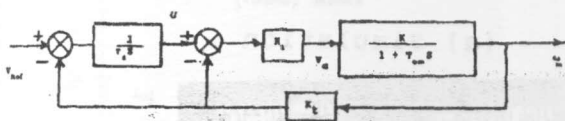


Figure 6. Complete block diagram for closed loop system.

This method of designing and calculating the speed P.I. controller parameters has the advantage of being straightforward, simple and accurate. The controller parameters are given in Appendix (2).

#### 4.3 Controller Equation

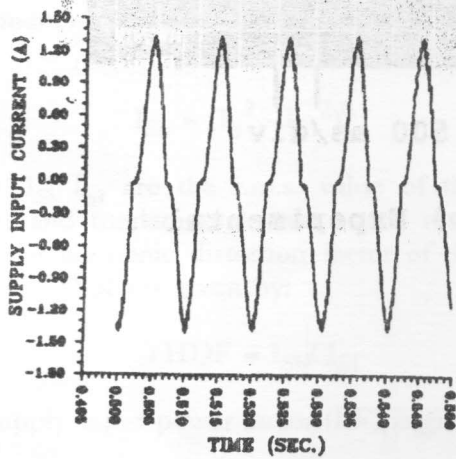
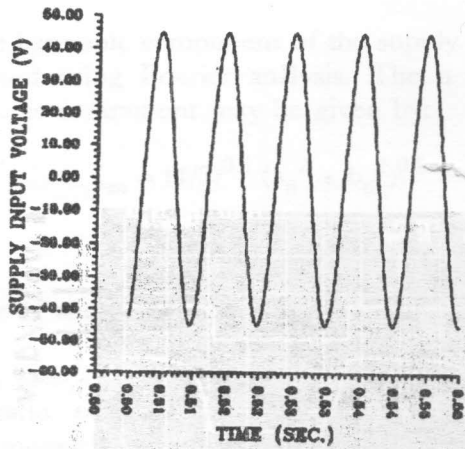
The controller equation is given as follows:

$$\tau_1 (d U / dt) = V_{Ref} - K_t \omega_m \quad (32)$$

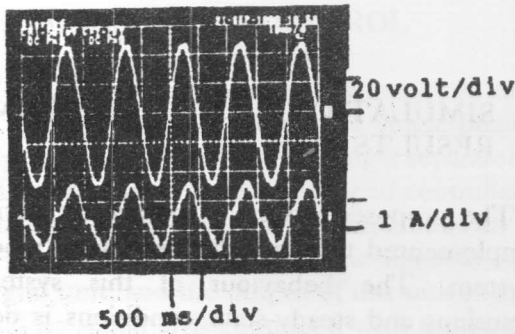
$$V_c = K_1 (U - K_t \omega_m) \quad (33)$$

### 5. SIMULATION AND EXPERIMENTAL RESULTS

The proposed system is practically designed and implemented to verify the developed model of this system. The behaviour of this system under transient and steady-state conditions is determined by solving the nonlinear differential equations using the fourth order Runge-Kutta method. The instantaneous and r.m.s. values of supply input current and voltage, motor current and voltage, developed torque and motor speed are obtained from the proposed numerical simulation. The open loop and closed loop behaviour of this system show the accuracy of the developed simulation.

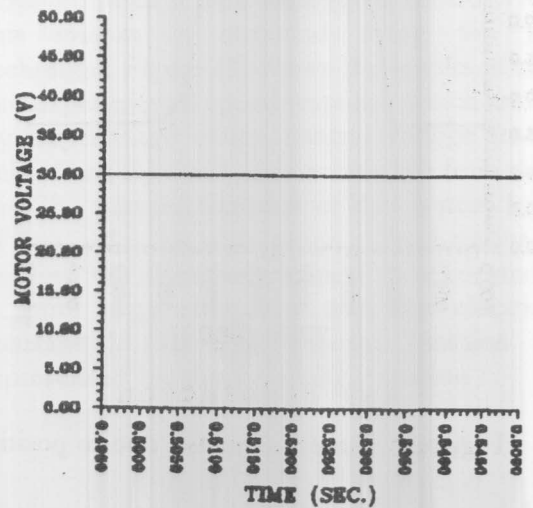
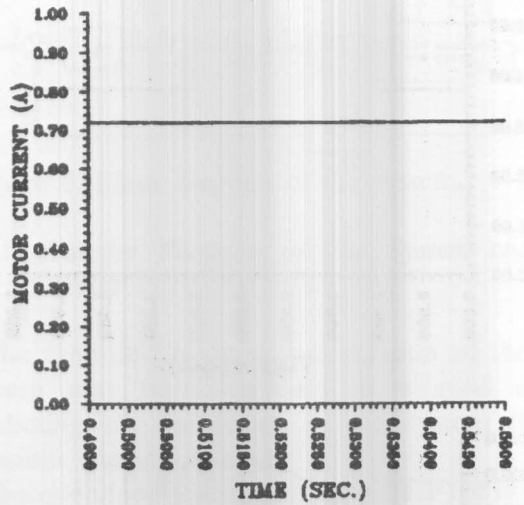


(a) Simulation .

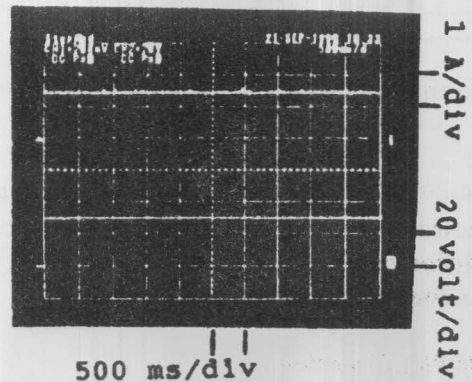


(b) Experimental .

Figure 7. Simulation and experimental results for supply input voltage and current waveforms.



(a) Simulation .



(b) Experimental .

Figure 8. Simulation and experimental results for motor voltage and current.



5.1 Open Loop System

Figure (7) shows the predicted and experimental results of supply input current and voltage waveforms. Figure (8) shows the predicted and experimental results of motor voltage and current. These results are taken for a control voltage of 8 volt and a load torque of 1/2 full load. It can be seen that the supply current is nearly sinusoidal. Also, it can be detected from Figure (8) that the dc input voltage and current are reasonably ripple free.

Figures (9,10) show the variation of total harmonic distortion factor (THDF) and power factor versus control voltage. It can be seen from Figure (9) that the control voltage highly affects the value of THDF. Figure (10) shows that the supply input power factor is almost close to unity and increases with the increase of load torque. This may be attributable to the decrease of THDF due to increase in motor d.c. current with respect to harmonic contents.

was made at about  $\pm 25\%$  of the existing load torque.

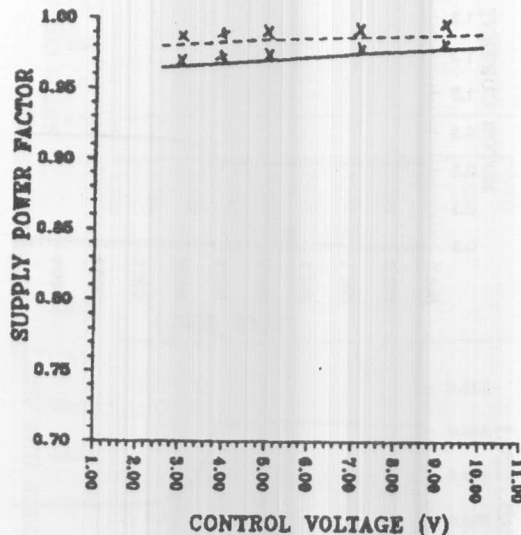


Figure 10. Power factor versus control voltage.

— 0.5 Full load.  
 .... Full load.  
 XXXX Experimental results.

5.2 Closed Loop system

Figure (13) shows the computed and experimental response of motor speed due to step change in the reference voltage at half full-load. It is clear that the motor can follow the desired speed reference smoothly with a reasonable overshoot.

Figure (14) shows the computed and experimental results for motor current and speed response due to step change in input voltage at half full-load. The step change was made at about  $\pm 15\%$  of the rated voltage. The results illustrate that the motor current and speed changes according to the change of input voltage and then they return to their initial steady-state values.

Figure (15) shows the computed and experimental variation of speed and current due to positive and negative change (similar to those of open loop) in the existing load. It is clear from the Figure that, the speed has returned to its initial value after 400 m sec which in turn confirms the validity of the proposed system.

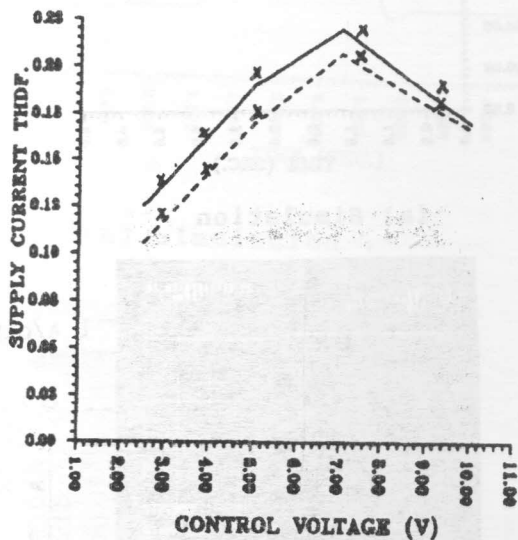
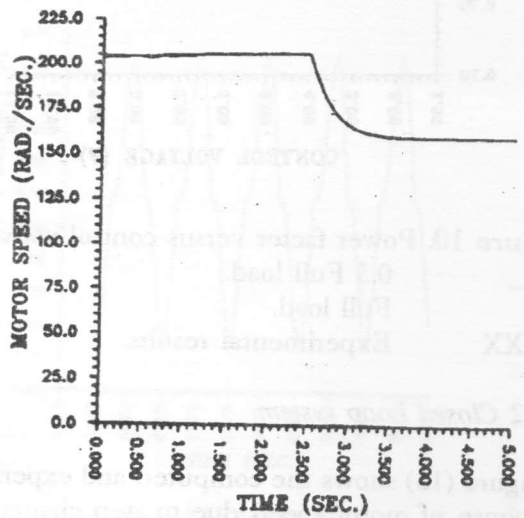
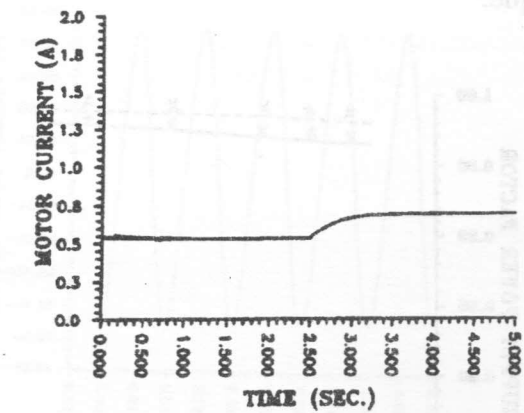


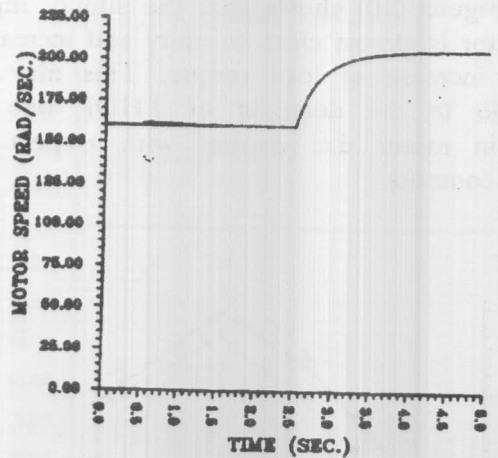
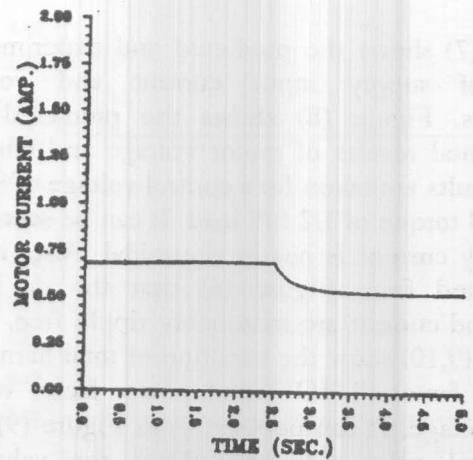
Figure 9. Total harmonic distribution factor versus control voltage with

— 0.5 full load.  
 ..... Full load.  
 XXXX Experimental results.

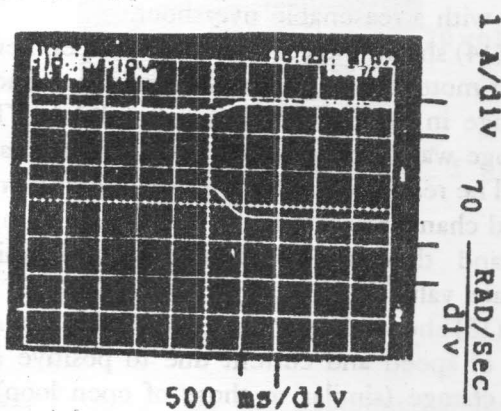
Figures (11,12) show the computed and experimental results for positive and negative step change in load torque respectively. The step change



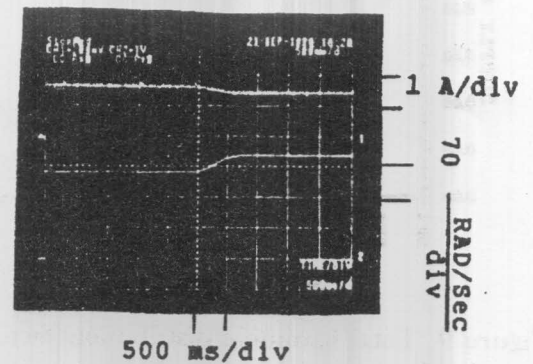
(a) Simulation .



(a) Simulation .



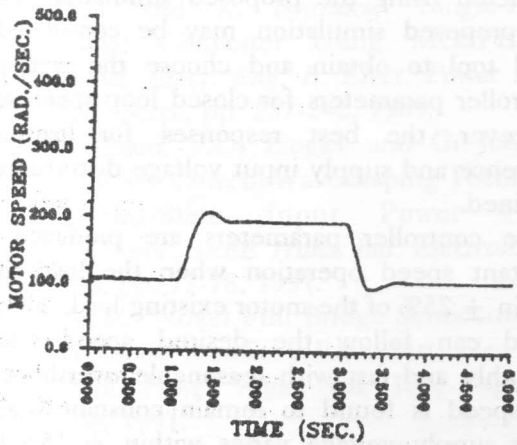
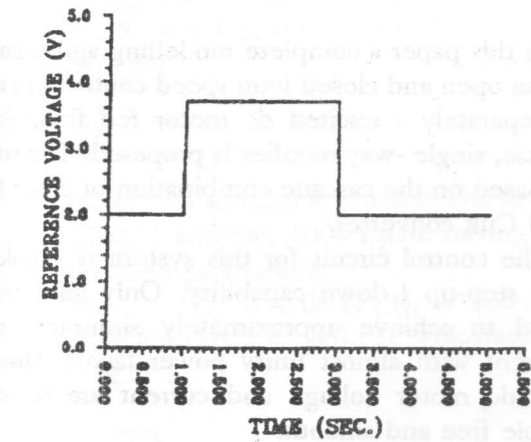
(b) Experimental .



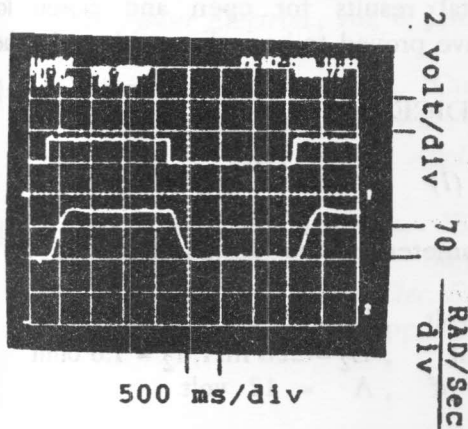
(b) Experimental .

Figure 12. Variation of speed due to negative step change for open loop system.

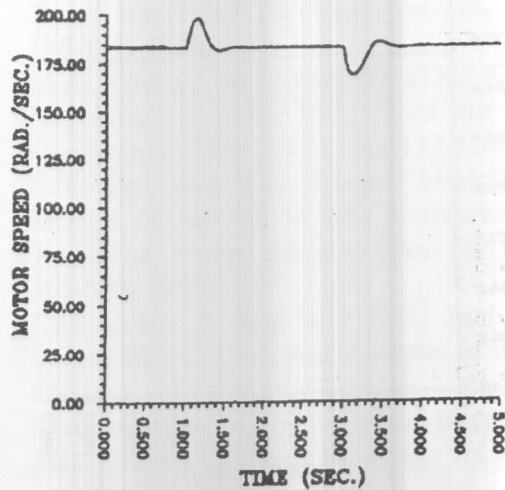
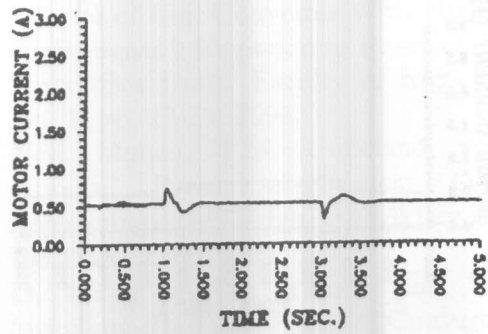
Figure 11. Variation of speed due to positive step change for open loop system.



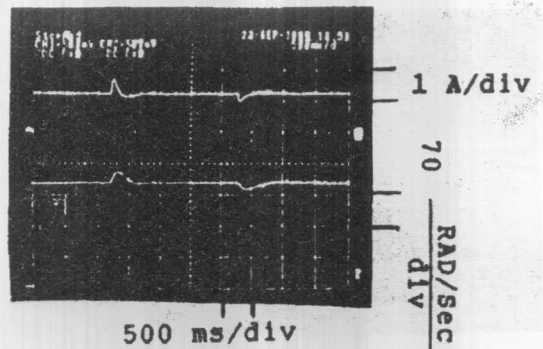
(a) Simulation .



(b) Experimental .



(a) Simulation .



(b) Experimental .

Figure 14. Variation of current and speed due to positive and negative step change of supply voltage for closed loop system.

Figure 13. Variation of speed due to positive and negative step change of reference voltage for closed loop system.

6. CONCLUSIONS

In this paper a complete modelling and simulation of an open and closed loop speed control scheme for a separately - excited dc motor fed from single - phase, single -way rectifier is proposed. The strategy is based on the cascade combination of diode bridge and Cuk converter.

The control circuit for this system is simple, and has step-up / down capability. Only one switch is used to achieve approximately sinusoidal supply current with almost unity power factor. Moreover, the dc motor voltage and current are reasonably ripple free and smooth.

The dynamic and steady-state behaviour are predicted using the proposed simulation. Further, the proposed simulation may be considered as a good tool to obtain and choose the suitable P.I controller parameters for closed loop speed control. However, the best responses for load, speed reference and supply input voltage disturbances are obtained.

The controller parameters are predicted for a constant speed operation when the load changes within  $\pm 25\%$  of the motor existing load. The motor speed can follow the desired speed reference smoothly and fast with reasonable overshoot. Also, the speed is found to remain constant when the input supply voltage varies within  $\pm 15\%$  of the applied voltage.

The comparison between simulation and experimental results for open and closed loop systems have proved to be in line with each other.

7. APPENDICES

Appendix (1)

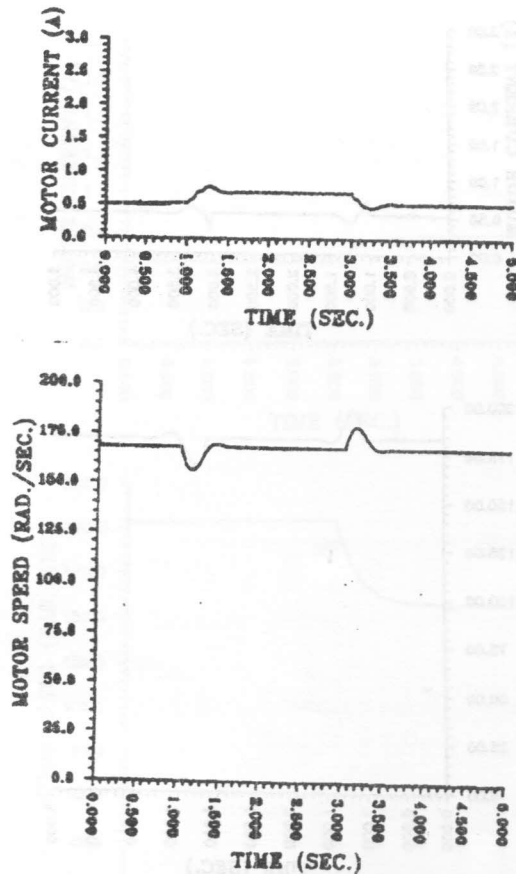
The parameter of the designed system are as follows:

$$\begin{aligned}
 v_s &= 45 \text{ volt} & , L_1 &= 25 \text{ mH}, r_1 = 1.6 \text{ ohm} \\
 C &= 5 \text{ uf} & , L_2 &= 220 \text{ mH}, r_2 = 1.6 \text{ ohm} \\
 C_o &= 1200 \text{ uf} & , A &= 12 \text{ volt}
 \end{aligned}$$

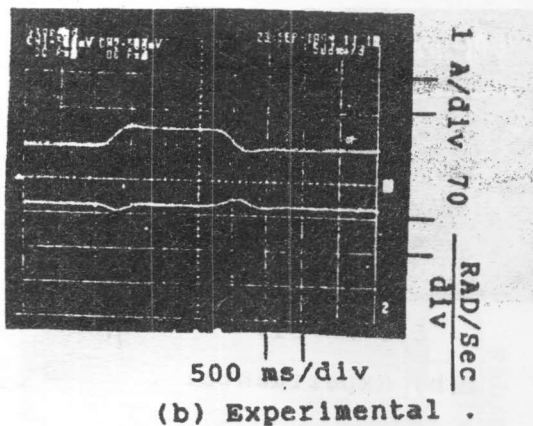
Appendix (2)

The values of P.I. speed controller parameter are as follows:

$$R_3 = 30 \text{ ohm} \quad , R_4 = 50 \text{ ohm} , R_5 = 50 \text{ ohm},$$



(a) Simulation.



(b) Experimental .

Figure 15. Variation of current and speed due to positive and negative step change of load torque for closed loop system.



$$C_1 = 3.3 \text{ uF}, V_{\text{Ref}} = 2 \text{ volt}, K_t = 0.019 \text{ volt/rad/sec.}$$

$$K = 10.0, K_1 = 1.0, \tau_1 = 0.07 \text{ sec.}$$

$$T_{c m} = 0.087 \text{ Sec.}$$

### Appendix (3)

The test motor is a separately excited DC motor, 50 volt, 50 watt, 1 ampere, 3000 r.p.m. having the following measured parameters:

$$R_a = 10.5 \text{ ohm}, L_a = 0.06 \text{ H}, R_f = 550 \text{ ohm}$$

$$B = 0.0001 \text{ N.m./rad/sec}, k_m = 0.127 \text{ Volt/(rad/sec)}$$

$$J = 0.0012 \text{ kg.m}^2.$$

### 8. REFERENCES

- [1] R. Itoh and K. Ishizaka, "Single-Phase Sinusoidal Converter Using MOSFET'S", *Proc. Inst. Elect. Eng. B. Elect. Power Appl.*, vol. 136, Setp., pp. 237-242, 1989.
- [2] M. Kazerani, P.D. Ziogas, and G. Joos, "A Novel Active Current Waveshaping Technique for Solid-State Input Power Factor Conditioners", *IEEE Trans. Ind. Electron.*, vol. 38, Feb. pp. 72-78, 1991.
- [3] S. Manias, "Novel Full Bridge Semicontrolled Switch mode rectifier", *Proc. Inst. Elec. Eng. B. Elect. Power Appl.*, vol. 138, Sept. pp. 252-256, 1991.
- [4] A.r. Prasad, P.D. Ziogas, and S. Manias, "An Active Power Factor Correlation Technique for Three-Phase Diode Rectifiers", *IEEE Trans. Power Electron.*, vol. 6, Jan. pp. 83-92, 1991.
- [5] J.T. boys and A.W. Green, "Current-Force Single-Phase Reversible Rectifier", *Proc. Inst. Elec. Eng. b. Elect. Power Appl.*, vol. 136, Sept. pp. 205-211, 1989.
- [6] R. Itoh and K. Ishizaka, "Single-Phase Sinusoidal Rectifier with Step-Up/Down Characteristics", *Proc. Inst. Elec. Eng. B. Elect. Power Appl.*, vol. 138, Nov. pp. 338-344, 1991.
- [7] A.E. Lashine and F.A. Saafan, "Analog Control of Cuk Converter With High Quality Performance", *Engineering Research Bulletin, Menoufiya Univ., Faculty of Eng.*, vol. 19, No. 1, pp. 17-33, 1996.
- [8] Ned. Mohan, T.M. Undeland, and W.P. robbins, *Power Electronics: Converters, Applications and Design*, John Wiley and Sons. Inc. New York, 1989.
- [9] D. Weng and S. Yuvara Jan, "Constant Switching-Frequency AC-DC Converter Using Second-Harmonic-Injected PWM", *IEEE Trans. on Power Electron.*, vol. 11, Jan. pp. 115-121, 1966.
- [10] M.A. Ghazy, "A Novel DC/DC Switching Regulator", *Al-Azhar Eng. Third International Conference*, Dec. 18-21, pp. 117-128, 1993.
- [11] C.T. Pan and T.C. Chen, "Modelling and Design of An AC to DC Converter", *IEEE Trans. on Power Electron.*, vol. 8, Oct. pp. 501-508, 1993.
- [12] J.W. Kolar, A. Ertl and F.C. Zach, "Space Vector-Based Analytical Analysis of the Input Current Distortion of a three-phase Discontinuous-Mode Boost Rectifier System", *IEEE Trans. on Power Electron.*, vol. 10, Nov. pp. 733-745, 1995.
- [13] A.E. Emanuel and K.K. Sen, "Steady-State Performance of the DC Motor Supplied From Single-Phase Rectifier With Step-Up Converter A Unity Power Factor Converter", *IEEE Trans. on Energy conversion*, vol. 3, No.1, March, pp. 172-178, 1988.
- [14] P.c. Sen, *Thyristor DC Drives*, 1981 by John Wiley and Sons, Inc. United States of America.